

45, 2004 (1980); L. Dolan, Phys. Lett. **99B**, 344 (1981).

⁸Speculation about infinite parameter algebras in two-dimensional field theories has appeared in Dolan and Roos, Ref. 6; B. Julia, Ecole Normale Supérieure Report No. LPTENS 81-14, 1981 (to be published), and private communication. See also T. Curtright and C. Zachos, Phys. Rev. D **21**, 411 (1980), and University of Florida Report No. UFTP 80-19, 1980 (unpublished).

⁹See M. Adler and P. v. M. Moerbeke, Adv. Math. **38**, 267 (1980), and references therein.

¹⁰L. D. Faddeev, to be published.

¹¹Note that the general n th transformation has been explicitly defined for arbitrary field configurations (not just field solutions) and shown [see Eq. (14)] to shift $\mathcal{L}(x)$ by a total divergence. *Note added.*—I have recently received papers in which these transformations have been encapsulated in a generating function. See B. Hou, M. Ge, and Y. Wu, State University of New York at Stony Brook Report No. ITP-SB-81-28 (unpublished); C. Devchand and D. B. Fairlie, "A Generating Function for Hidden Symmetries of Chiral Models," to be published.

Higher-Order Effects in Wide-Angle Bremsstrahlung

Charles Chahine

Laboratoire de Physique Corpusculaire, Collège de France, F-75231 Paris, France

(Received 30 March 1981)

The origin of the large higher-order effects in radiative corrections is traced to charged-lepton scattering. The long radiative tail of the one-photon inclusive cross section, which does not arise in lowest order, is responsible for these large effects.

PACS numbers: 13.60.Hb, 13.40.Ks

Nonperturbative methods for radiative corrections, initiated in the basic work of Yennie, Frautschi, and Surra,¹ have been further developed in the important paper of Grammer and Yennie.² On the other hand, the more rigorous aspects of the nonperturbative treatment of infrared divergences have been vigorously studied by Zwanziger.³ Recently^{4,5} I have introduced rigorous and practical nonperturbative methods to effect radiative corrections. Surprisingly, these methods predicted⁵ that in the recent muon scattering experiments⁶⁻⁸ the elastic contribution is much larger, in the very inelastic regime, than the conventional one-emitted-photon (1γ) bremsstrahlung cross section.⁹ The choice of a technique to carry out the radiative corrections affects substantially the extracted nonradiative structure functions and in particular the scaling violations for small x . It is thus important to understand and possibly check by experiment

which approach is correct.

It is shown in this paper that these large higher-order effects⁵ originate from a long radiative tail to the *hard bremsstrahlung cross section*, not present if only one-photon emission is taken into account.¹⁰ In effect, in the very inelastic regime, there is a large probability that the hard photon is accompanied by collinear radiation. I compute this "radiatively corrected" hard bremsstrahlung cross section as a function of the photon energy and compare it to the conventional Bethe and Heitler¹¹ formula. The two results may be submitted to experimental test.

In the one-photon exchange approximation the bremsstrahlung differential cross section (DCS) in charged lepton-proton scattering, including the emission of an arbitrary number of collinear unobserved photons from the lepton vertex and the corresponding infrared virtual corrections, is given by

$$\frac{\omega d\sigma}{d\Omega' dE' d\omega} = \frac{\alpha^3}{(2\pi)^2} \frac{p'}{p} \int \frac{d^4q}{(q^2)^2} d\Omega_k W_j^{\text{NR}}(P, q) T_j(p, p'; k) \hat{E}(p, p'; p - q - p' - k). \quad (1)$$

Here, $P(M, 0)$, $p(E, \vec{p})$, $p'(E', \vec{p}')$, $k(\omega, \vec{k})$, and $q(q^0, \vec{q})$ are the momenta of the proton, the incident and scattered lepton, and the observed and exchanged photon, respectively; the vectors \vec{p}' and \vec{k} point in the solid angles Ω' and Ω_k . W_j^{NR} denotes the usual nonradiative proton structure functions ($j=1, 2$),

T_j , the lepton tensor components,^{5,9} and \hat{E} the infrared-free spectral function,^{5,12}

$$\hat{E}(p, p'; K) = (\alpha\bar{A})^2 e^{\alpha\hat{F}(r)} \int_0^\infty d\sigma \int_0^\infty d\sigma' (\sigma\sigma')^{-1+\alpha\bar{A}} \delta^4(K - \sigma l - \sigma' l'). \quad (2)$$

At high energies, the "infrared exponent" $\alpha\bar{A}$ and the normalization function $\alpha\hat{F}$ are given by

$$\alpha\bar{A} \simeq (\alpha/\pi) [\ln(Q_E^2/m^2) - 1], \quad (3a)$$

$$\alpha\hat{F} \simeq (\alpha/\pi) [\ln(Q_E/m) - \frac{1}{6}\pi^2]. \quad (3b)$$

Here α is the fine-structure constant, m is the lepton mass, $Q_E^2 = -(p - p')^2$ is the experimental square of the momentum transfer, and $r \simeq m^2/Q_E^2$. The light-cone momenta l and l' reduce to p and p' at high energies. In lowest-order perturbation theory, the differential cross section¹¹ (DCS⁰) is obtained from Eq. (1) by the substitution $\hat{E} \rightarrow \delta^4(p - q - p' - k)$.

Using Eq. (2) in (1) and effecting the q integration, we see that there remain two extra integrations over the parameters σ and σ' which appear in

$$q = l(1 - \sigma) - l'(1 + \sigma') - k. \quad (4)$$

$$\frac{d\sigma}{d\Omega' dE' d\omega} = \frac{\alpha^3}{(2\pi)^2} \frac{p'}{p} (\alpha\bar{A})^2 e^{\alpha\hat{F}} \int_D \frac{d\sigma d\sigma'}{(\sigma\sigma')^{1-\alpha\bar{A}}} \hat{W}_j(t) T_{j(1)} \frac{M}{\mu}, \quad (6)$$

where $2\pi T_{j(1)} = \int_0^{2\pi} d\varphi_k T_j$ are given explicitly in the appendix of Ref. 5 and the integration domain D is characterized by

$$A_- \leq (1 - \sigma)(1 + \sigma') \leq A_+, \quad \sigma \geq 0, \quad \sigma' \geq 0, \quad (7a)$$

where

$$A_\pm = \frac{t}{Q_E^2} \left(1 - \frac{\omega}{M} \right) \pm \frac{\omega\sqrt{t}}{Q_E^2} \left(\frac{t}{M^2} + 4 \right)^{1/2} \quad (7b)$$

and t is a linear function of σ and σ' which, from Eqs. (5), reads

$$\sigma\bar{E} + \sigma'\bar{E}' = E - E' - \omega - t/2M \equiv X. \quad (8)$$

Equations (7) and (8) lead to a pair of fourth-degree inequalities which are difficult to solve. Instead, we set

$$\sigma = X(1 - \tau)/\bar{E}, \quad \sigma' = X\tau/E', \quad (9)$$

and choose t and τ ($0 \leq \tau \leq 1$) as new integration variables in Eq. (6). We note that in lowest-order perturbation theory, $X \equiv 0$ and thus

$$t = t^0 = 2M(E - E' - \omega). \quad (10)$$

In the (t, ω) plane, the boundary curves are easily derived from Eq. (7) by setting $\tau = 0$ or $\tau = 1$. Figure 1 illustrates the results for a very inelastic kinematical configuration in which E

The azimuthal φ_k integration can be analytically effected by taking $\vec{u} = \vec{l}(1 - \sigma) - \vec{l}'(1 + \sigma')$ as polar axis in the laboratory frame. In the very inelastic regime, the bremsstrahlung cross section is dominated by the elastic contribution in which $W_{jel}^{NR} = 2M\hat{W}_j(t)\delta(w^2 - M^2)$, where M is the nucleon mass,

$$t \equiv -q^2 = \bar{Q}^2 + 2\omega(\Delta E - \mu \cos\theta_k), \quad (5a)$$

$$w^2 = (P + q)^2 = M^2 + 2Mq^0 - t, \quad (5b)$$

and the \hat{W}_j functions are readily expressed in terms of the nucleon form factors. Here, $\bar{Q}^2 = Q_E^2(1 - \sigma)(1 + \sigma')$, $\Delta E \equiv \mu_0 = \bar{E}(1 - \sigma) - \bar{E}'(1 + \sigma')$, where \bar{E} and \bar{E}' are the laboratory-energy components of l and l' , and θ_k is the polar angle of \vec{k} . With use of $\delta(w^2 - M^2)$ to effect the θ_k integration, Eq. (1) becomes

$= 270$ GeV, $Q_E^2 = 18.68$ GeV², and $x_E = Q_E^2/2\nu_E = 0.04$, where $\nu_E = M(E - E')$ in $\mu + p$ scattering. Curves (1) and (3) correspond to $\sigma' = \tau = 0$, curves (2) and (4) to $\sigma = 1 - \tau = 0$, and the "straight line" (note the semilogarithmic scale) to $\sigma = \sigma' = X = 0$. The physically important parameters defined with reference to lowest-order perturbation theory

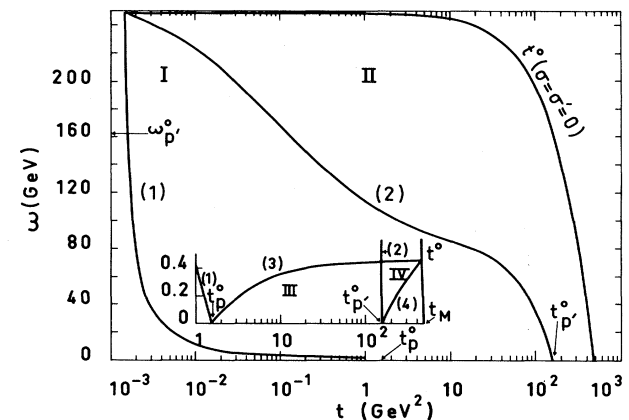


FIG. 1. Phase space boundary in the (t, ω) plane in $\mu + p$ scattering for $E = 270$ GeV, $x_E = 0.04$, and $Q_E^2 = 18.68$ GeV². Curves (1) and (3) correspond to $\sigma' = 0$, curves (2) and (4) to $\sigma = 0$, and t^0 to 1γ emission.

are, in increasing order of magnitude, t_{\min}^0 , t_p^0 , $t_{p'}^0$, and t_M corresponding to the minimum, the "p peak," the "p' peak," and the maximum allowed value of t , respectively.¹³ The corresponding ω values are defined using Eq. (10) and denoted ω_{\max}^0 , ω_p^0 , $\omega_{p'}^0$, and ω_{\min}^0 . The effective part of D is split into four subdomains (I to IV), each one being delimited by three curves: I [(1), (2), (3)]; II [(2), (3), $t=t^0$]; III [(2), (3), $\omega=0$]; and IV [(2), (3), (4)]. For fixed t , the corresponding limits on the τ integration, derived from Eqs. (7), are $[0, \tau_{\max}]$, $[0, 1]$, $[\tau_{\min}, \tau_{\max}]$, and $[\tau_{\min}, 1]$, where

$$\tau_{\min}^{\max} = \frac{(X - \bar{E} - \bar{E}') + [(X - \bar{E} + \bar{E}')^2 + 4\bar{E}\bar{E}'A_{\mp}]^{1/2}}{2X}. \quad (11)$$

$$\frac{d\sigma}{d\Omega' dE' d\omega}$$

$$= \frac{\alpha^3}{(2\pi)} \frac{p'}{p} e^{\alpha\hat{F}(4M^2\bar{E}\bar{E}') - \alpha\bar{A}M(\alpha\bar{A})^2} \int_0^1 \frac{d\tau}{[\tau(1-\tau)]^{1-\alpha\bar{A}}} \int_{t_{\text{in}}(\tau)}^{t^0} \frac{dt}{(t^0-t)^{1-2\alpha\bar{A}}} \frac{\hat{W}_i(t) \mathcal{T}_i(\omega, t, \tau)}{\mu t^2}, \quad (12)$$

where $t_{\text{in}}(\tau)$ is the inverse function of $\tau_{\max}(t)$ given in Eq. (11). In practical computations, $t_{\text{in}}(\tau)$ is obtained as the solution of a fourth-degree equation with $t_1 \leq t_{\text{in}}(\tau) \leq t_2$, where t_1 and t_2 correspond to curves (1) and (2). Equation (12) is the central formula of this paper. To recover perturbation theory, it is convenient to think of one factor $\alpha\bar{A}$ as associated with the "singularities" at $\tau=0$ or $\tau=1$, the other factor $\alpha\bar{A}$ being associated with the singularity at $t=t^0$.

Figure 2 illustrates the hard bremsstrahlung differential cross section from Eq. (12) in $\mu+p$ scattering compared to DCS^0 for $E=280$ GeV, $Q_E^2=5.0$ GeV², and $x_E=0.01$ (curves *a*) and $x_E=0.1$ (curves *b*) with use of the standard dipole proton form factors. It is important to realize that the log-log scale used to resolve the peak located very closely to ω_{\max}^0 overemphasizes the peak region with respect to the tail where in fact most of the integrated cross section lies. This figure shows that DCS and DCS^0 resemble a "hadronic" cross section, with and without radiative corrections, respectively. The fundamental result of this paper is that this tail becomes very long for small x_E and large Q_E^2 as curve *a* shows. This result may also have been qualitatively anticipated from Fig. 1.

Let us define CS_{peak} and CS_{tail} as the ω -integrated cross section in the $[\omega_p^0, \omega_{\max}^0]$ and $[\omega_{\min}^0, \omega_p^0]$ intervals, respectively, with parallel definitions for $\text{CS}_{\text{peak}}^0$ and $\text{CS}_{\text{tail}}^0$. The values of

Since in lowest order of standard perturbation theory $\omega_{\min}^0 \leq \omega \leq \omega_{\max}^0$, the part of the higher-order spectrum below ω_{\min}^0 involves the emission of at least two real photons. Also, since the t values are quite large for this part of the spectrum (see the inset in Fig. 1) DCS is suppressed by $1/t^2$ and by the nucleon form factors. We note, however, that a rise in DCS will occur for a soft *observed* photon energy corresponding to a $d\omega/\omega$ spectrum at order α^4 . For simplicity and relevance to a recent experiment where only hard photons are measured,¹⁴ I have computed in this program DCS for $\omega \geq \omega_{\min}^0$ where only subdomains I and II are relevant.

Computing the Jacobian for the $(\sigma, \sigma') \rightarrow (t, \tau)$ change of variables, and lumping together subdomains I and II, Eq. (6) becomes

these cross sections are indicated in Table I for the two kinematical configurations of Fig. 2. For very inelastic scattering, $x_E=0.01$, we see that although DCS in the tail region is about 4 orders of magnitude smaller than its peak value, CS_{tail} is 6 times *larger* than CS_{peak} . Indeed, the tail extends over 260 GeV whereas the peak extends over 0.12 GeV only. The very large difference be-

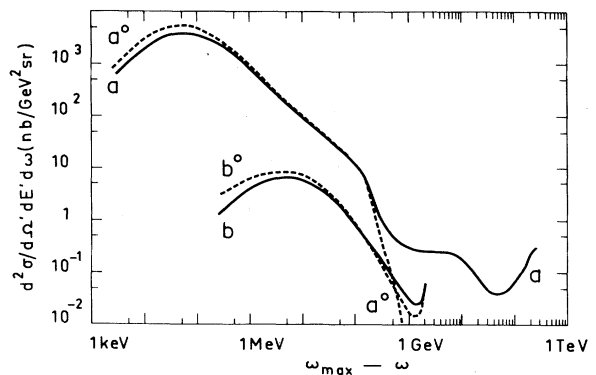


FIG. 2. Bremsstrahlung differential cross section in $\mu+p$ scattering at $E=280$ GeV, $Q_E^2=5.0$ GeV². Curves *a* are for $x_E=0.01$ where $t_{\min}^0=8.9 \times 10^{-5}$ GeV², $\omega_{\max}^0=266.439$ GeV, $\omega_p^0=266.315$ GeV, $\omega_{\min}^0=0.46$ GeV; and curves *b* are for $x_E=0.1$ where $t_{\min}^0=9.7 \times 10^{-4}$ GeV², $\omega_{\max}^0=26.639$ GeV, $\omega_p^0=24.211$ GeV, $\omega_{\min}^0=0.41$ GeV. Solid curves are for DCS and dashed curves for DCS^0 .

TABLE I. ω -integrated bremsstrahlung cross sections in units of nb/GeV sr. $E = 280$ GeV, $Q_E^2 = 5.0$ GeV².

x_E	CS_{peak}	CS_{peak}^0	CS_{tail}	CS_{tail}^0
0.01	6.57	7.05	38.10	0.70
0.1	0.50	0.53	0.17	0.15

tween CS_{tail} and CS_{tail}^0 is not surprising since the radiative tail involves at least two-photon emission which considerably lowers the relevant t values, as seen in Fig. 1. For $x_E = 0.1$, the difference between the results given by first-order perturbation theory and the inclusion of higher-order effects is much less pronounced, since much less phase space is available for multiphoton emission.

Comparison of DCS and DCS^0 with experiment involves a "binning," that is, an integration over some hopefully small domain in x_E and Q_E^2 which will considerably spread the narrow peak predicted in both formulas. The radiative tail which, as we have seen, has a much lower cross section, spreads over a much larger range in photon energy. Its observation depends more on background and on the details of the experiment. It may be valuable to note that too sharp angular cuts on the photon direction may eliminate part if not all of the radiative tail. To illustrate this fact, we let θ_v denote the polar angle of $\vec{v} = \vec{p} - \vec{p}'$, and obtain for the kinematics of case a $\langle \theta_k \rangle = 3.8 \times 10^{-5}$ rad, $\langle \theta_v \rangle = 1.2 \times 10^{-10}$ rad at the peak, and $\langle \theta_k \rangle = 7.9 \times 10^{-4}$ rad, $\langle \theta_v \rangle = 1.3 \times 10^{-2}$ rad at $\omega = 33$ GeV.

The integrated cross section $CS^0 = CS_{\text{peak}}^0 + CS_{\text{tail}}^0$ is usually used by experimentalists to subtract from the data the elastic contributions to $d\sigma/d\Omega' dE'$. In the present nonperturbative approach to radiative corrections, the integrated cross section is related but not equivalent to the elastic contribution discussed in Ref. 5. In effect, I have shown in this reference that the "inclusive" cross section involves the contribution of zero and one oblique photon, and an oblique photon does not have, in contrast with an observed photon, a $d\omega/\omega$ spectrum because of the built-in counterterms. However, since soft photons are not very important for small x_E , the order of magnitude of these cross sections is the same. For the kinematics of case a , for example, I

found that the contribution of zero and one oblique photon is 5.7 and 53.5 nb/GeV sr, respectively, as compared with $CS = CS_{\text{peak}} + CS_{\text{tail}} = 44.7$ nb/GeV sr. Here, the higher-order elastic contribution is about 7 times CS^0 . These large effects are expected to be smoothed after binning and experimental cuts.¹⁴

In conclusion, this paper demonstrates that the long radiative tail to the hard bremsstrahlung in the very inelastic regime accounts almost trivially for the large higher-order effects reported previously.⁵ I urge the various experimental groups to take into account these effects in their analyses in order to clarify the scaling violations for small x_E and large Q_E^2 .

¹D. Yennie, S. Frautschi, and H. Suura, Ann. Phys. (N.Y.) **13**, 379 (1961).

²G. Grammer and D. R. Yennie, Phys. Rev. D **8**, 4332 (1973).

³D. Zwanziger, Phys. Rev. D **20**, 2011 (1979), and **11**, 3481, 3504 (1975).

⁴C. Chahine, Phys. Rev. D **22**, 1062 (1980).

⁵C. Chahine, Phys. Rev. D **22**, 2727 (1980).

⁶B. A. Gordon *et al.*, Phys. Rev. Lett. **41**, 615 (1978).

⁷R. C. Ball *et al.*, Phys. Rev. Lett. **42**, 866 (1979).

⁸J. J. Aubert *et al.*, in *High Energy Physics—1980*, edited by Loyal Durand and Lee G. Pondrom, AIP Conference Proceedings No. 68 (American Institute of Physics, New York, 1981).

⁹L. W. Mo and Y. S. Tsai, Rev. Mod. Phys. **41**, 205 (1969); Y. S. Tsai, SLAC Report No. PUB-848, 1971 (unpublished). Current procedures are described by G. Miller *et al.*, Phys. Rev. D **5**, 528 (1972). These methods are not equivalent to the present ones since they take into account higher-order effects to the basic scattering process (exponentiation or equivalent radiators method) but not to the hard bremsstrahlung as such.

¹⁰D. Yennie emphasized long ago that two-photon emission effects may be important. I thank Professor D. Yennie for fruitful and enjoyable discussions about this point and the Cornell University High Energy Physics group for their kind invitation during the summer of 1980.

¹¹H. Bethe and W. Heitler, Proc. Roy. Soc. London, Ser. A **146**, 83 (1934). See also W. Heitler, *The Quantum Theory of Radiation* (Oxford Univ. Press, London, 1936).

¹²C. Chahine, Phys. Rev. D **18**, 4617 (1978).

¹³See Eqs. (3.27), (3.29), and (3.40) of Ref. 4.

¹⁴I learned this from the European Muon Collaboration group who are in the course of implementing my programs in their analysis.